Available online at www.sciencedirect.com
SCIENCE DIRECT
Journal of the European Ceramic Society 26 (2006) 1075–1084
www.elsevier.com/locate/jeurceramsoc

Application of the acoustic emission technique to characterise liquid transfer in a porous ceramic during drying

T. Chotard [a, b, *], A. Quet [a], A. Ersen [a], A. Smith [a]

[a] *Groupe d'Etude des Matériaux Hétérogènes (GEMH, EA 3178) Ecole Nationale Supérieure de Céramique Industrielle, 47 à 73 Avenue Albert Thomas, 87065 Limoges Cedex, France*
[b] *Institut Universitaire de Technologie, Département Génie Mécanique et Productique, 2 allée André Maurois, 87065 Limoges Cedex, France*

Received 9 September 2004; received in revised form 6 January 2005; accepted 10 January 2005
Available online 31 March 2005

Abstract

In this paper, some aspects of the characterisation of liquid transfer during drying process of a porous ceramic by acoustic emission (AE) technique are presented and discussed. Results are compared with the general theory of drying and a recent approach dealing with thermodynamic modelling based on capillary stresses and hygromechanical coupling. The sensitivity of the acoustic emission technique to the energy release processes acting during liquid transfer in a porous material (sorption and desorption) has been emphasised. Based on the experiments, the relationship between the AE characteristics recorded during the tests and the different mechanisms, which take place during drying process, was underlined. Information deduced from AE measurements associated with other data obtained from weight-loss measurements enable to propose a qualitative description of drying chronology. The results show that this new application of the AE technique could be considered as a valuable tool to study the liquid transfer in a porous material.

Keywords: Drying; Acoustic emission

1. Introduction

Drying in ceramic processes, removal of water in clays or consumption of water through hydration of cementitous materials, are situations where liquid transport processes in porous media are involved.[1–5] Understanding how liquid flows through a porous body is an issue that has been studied academically in many different fields: soil mechanics,[6] saturated porous media for oil prospecting[7] or storage of polluting agents.[8–10] Recent work concerns the characterisation of transfer moisture in building materials.[11–16] The experimental approaches that have been developed are mostly based on ultrasonic techniques.[17,18] In the present case, we have applied acoustic emission (AE). Indeed, this technique is sensitive to energy release phenomena that induce propagation of elastic waves in a material submitted, for example, to stresses. Example are on flaw formation and failure in structural materials submitted to compression or traction loads, leading to crack nucleation and propagation, phenomena of multiple dislocation slip, twinning, grain boundary sliding, Barkhausen effect (realignment or growth of magnetic domains), phase transformations in alloys, debonding of fibres in composite materials or fracture of inclusions in alloys.[19–23] In the case of cements or plasters hydration and setting, where drying is involved, data have shown that it is active in acoustic emission.[24]

This paper is devoted to the study by AE of water adsorption in a porous ceramic material and it's drying after impregnation with water. It is divided as follows: the different stages of drying, forces exerted on the solid and transport mechanisms within the liquid are developed in the second paragraph. The porous material and the acoustic emission technique are described in the third part. The results are divided into two sections: the first concerns wa-

* Corresponding author.
E-mail addresses: t_chotard@ensci.fr (T. Chotard), a_smith@ensci.fr (A. Smith).

0955-2219/$ – see front matter © 2005 Elsevier Ltd. All rights reserved.
doi:10.1016/j.jeurceramsoc.2005.01.048

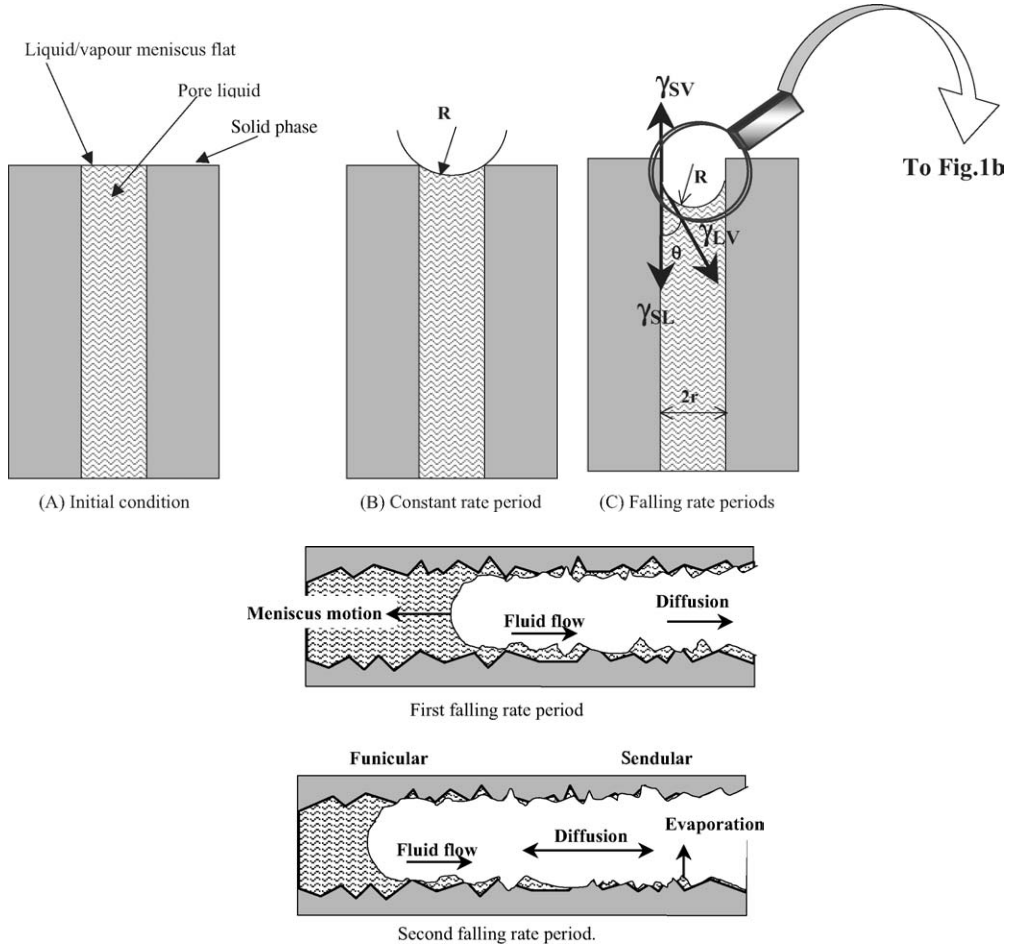

Fig. 1. (a) Schematic illustration of the general chronology of drying process for a pore. (b) Details about the first and second falling rate periods (from Scherer[25]).

ter adsorption experiments and the second presents drying tests.

2. General theory of drying

The principle of flow in porous bodies is relatively simple but its analysis is rather complicated.[25] Liquid flows through a porous medium in response to a gradient in pressure. At the same time, the pressure induces deformation of the solid skeleton and dilatation of the pores through which the liquid moves. To better understand the chronology of drying, stages and driving forces involved in the process are detailed below.

2.1. Chronology of stages

Considering a porous medium saturated with a liquid, the drying process can be divided into three periods, as illustrated in Fig. 1.

The first stage, called the constant rate period (Fig. 1a, part B), is when evaporation occurs only from the surface of the pore. During this stage, the rate of evaporation per unit area of the drying surface is independent of time and is the same as for a free water surface. The liquid/vapour interface, or meniscus, remains at the exterior surface of the body but its radius decreases continuously, due to evaporation. The liquid is in tension and the solid phase is in compression, which may cause shrinkage in deformable systems. At the end of this period, called the critical point, the radius of the meniscus becomes equal to the radius of the pore and the compressive forces exerted on the solid are at the maximum.

The second step is called the first falling rate period (Fig. 1b). Just beyond the critical point, the radius of curvature of the meniscus is small enough to enter the pores and the liquid recedes into the pores. During this period, the rate of evaporation decreases and is sensitive to the ambient temperature and vapour pressure. Compressive forces, and consequently shrinkage, in deformable solids, virtually stop. The liquid in the pores located near the surface flows to the outside and evaporates from the external surface. At the same time, part of the liquid can evaporate within the pores and the vapour is diffused to the surface. This situation is characterised by coupled effects, namely liquid flow and diffusion of vapour.

The third stage is called the second falling rate period (Fig. 1b). As drying progresses, some of the liquid water cannot reach the surface (due to the deep penetration of the liquid meniscus in the porous network) and has to evaporate within the pores. As the saturated area retracts into the body, the solid skeleton is submitted to differential strains induced by a gradient of stress in the medium (compression in the saturated region is higher than near the drying surface).

2.2. Forces on the solid and transport mechanisms of the liquid

Several forces can induce stresses on the solid body during the drying process:

- *The capillary pressure*. During the first stage of drying, the capillary pressure, P_c in the liquid, is directly related to radius of curvature (R) of the meniscus through *Laplace's law*:

$$P_c = \frac{-2\gamma_{LV}}{R} \tag{1}$$

where γ_{LV} is the liquid/vapour interfacial energy (or surface tension). The sign of the capillary pressure is related to the sign of the radius of curvature. When the centre of curvature is located in the vapour phase, R is negative, P_c is positive and the liquid is in tension. The maximum capillary pressure (P_R) occurs when R is sufficiently small to enter the pore. The minimum value of R for a cylindrical pore with a radius r is given by:

$$R = -\frac{r}{\cos\theta} \tag{2}$$

where θ is the contact angle representing the wetability of the liquid. For real pores (non-cylindrical), P_R is related to the surface-to-volume ratio of the pore space S_P/V_P:

$$P_R = \frac{(\gamma_{SV} - \gamma_{SL})S_P}{V_P} = \frac{\gamma_{LV}\ \cos\theta\ S_P}{V_p} \tag{3}$$

where γ_{SV} and γ_{SL} are the solid/vapour and solid/liquid interfacial energies. When examining the surface-to-volume ratio of the pore, we can see that it is related to the specific surface area of a porous body by:

$$\frac{S_P}{V_P} = \frac{S\rho_s\rho}{1-\rho} \tag{4}$$

where ρ is the relative density, $\rho = \rho_b/\rho_s$, ρ_b is the bulk density of the solid network (not considering the mass of liquid) and ρ_s is the density of the solid skeleton.

We will see in the following of this study that this surface-to-volume ratio of the pore has a notable importance to explain the chronology of drying.

- *The moisture stress*. This stress also called moisture potential, is the partial specific Gibbs free energy of a liquid in a porous medium:

$$G = \left(\frac{R_g T}{\rho_L V_m}\right) \ln\left(\frac{p_v}{p_0}\right) \tag{5}$$

where ρ_L and V_m are the density and the molar volume of the liquid, R_g is the ideal gas constant, T is the temperature, p_v is the vapour pressure of the liquid in the system and p_0 is the vapour pressure over a flat surface of the pure liquid.

Two other driving forces can be also considered: the osmotic pressure which is produced by a concentration gradient in the liquid and the disjoining pressure dealing with short-range forces resulting from the presence of a solid/liquid interface. Analysis of these forces will not be developed here.

As we note in Section 2.1, two kinds of transport processes are involved during the falling rate period of drying: flow and diffusion.

Fluid flow through porous media follows *Darcy's law* which affirms that the flux of liquid, J, is proportional to the gradient in pressure in the liquid, ∇P_L:

$$J = -\frac{D}{\eta_L}\nabla P_L \tag{6}$$

where D is the permeability (in units of area), η_L is the viscosity of the liquid. The permeability D is also related, through the Carman–Kozeny equation, to the relative density and the specific surface area, already defined before:

$$D = \frac{(1-\rho)^3}{5(\rho S\rho_S)^2} \tag{7}$$

the factor of 5 is empirical and corrects the non-circular section of real pores.

During evaporation, a part of the vapour is transported by diffusion that obeys *Fick's law* where the diffusive flux (J_D) is proportional to the concentration gradient (∇C):

$$J_D = -D_c\nabla C \tag{8}$$

where D_c is the chemical diffusion coefficient and C the concentration.

3. Experimental procedure

3.1. Material

The porous material used in our work is a cylindrical silica–alumina sintered ceramic sample, with a diameter and a height of 100 and 10 mm, respectively. The porous characteristics have been measured by mercury porosimetry measurements (Autopores II micromeritics 9200). The cumulative open porous volume is of the order of 33 vol.%. The pore size ranges mainly between 70 and 80 μm and 200 and 300 μm and there is a small percentage of pores between 5 and 20 nm (Fig. 2). A micrograph by scanning electron microscopy (Cambridge S260) reveals that the large pores correspond to intergranular porosity while the small ones are

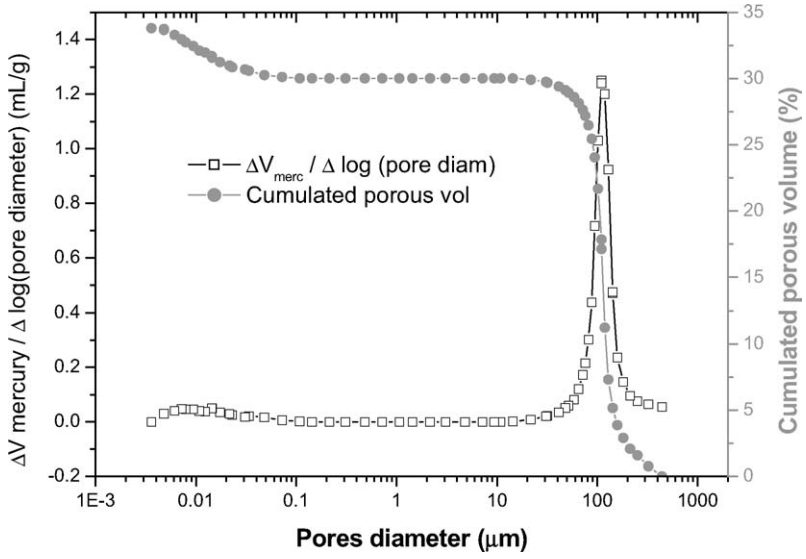

Fig. 2. Porous volume and pore size distribution of the porous ceramic.

within the grains (Fig. 3). Lastly, the porous network of micron size is rather tortuous. In order to study adsorption and drying phenomena, this porous material has been selected because it has a large porous volume and consequently, the surface developed by the interior of the pores is about 10^3 times greater than the outer surface of the ceramic.

3.2. Experimental set-up

The acoustic emission system used in this study is a AEDSP-32/16 MISTRAS digital system from Physical Acoustics Corporation. This system allows the waveform and the main feature parameters well known in AE study such as count, hit, rise time, duration of hit, count to peak, amplitude (in dB), to be recorded. Fig. 4 presents different AE features extracted from the signal waveform.

The plug-in filter of this system has a bandwidth from 100 to 1200 kHz. Two sensors (PAC MICROPHONE R15), one test sensor and one reference sensor, with a bandwidth from 50 to 250 kHz, are connected through preamplifiers (EPA 1220A). The reference sensor is used in order to record noises due to the electromagnetic environment and to eventually

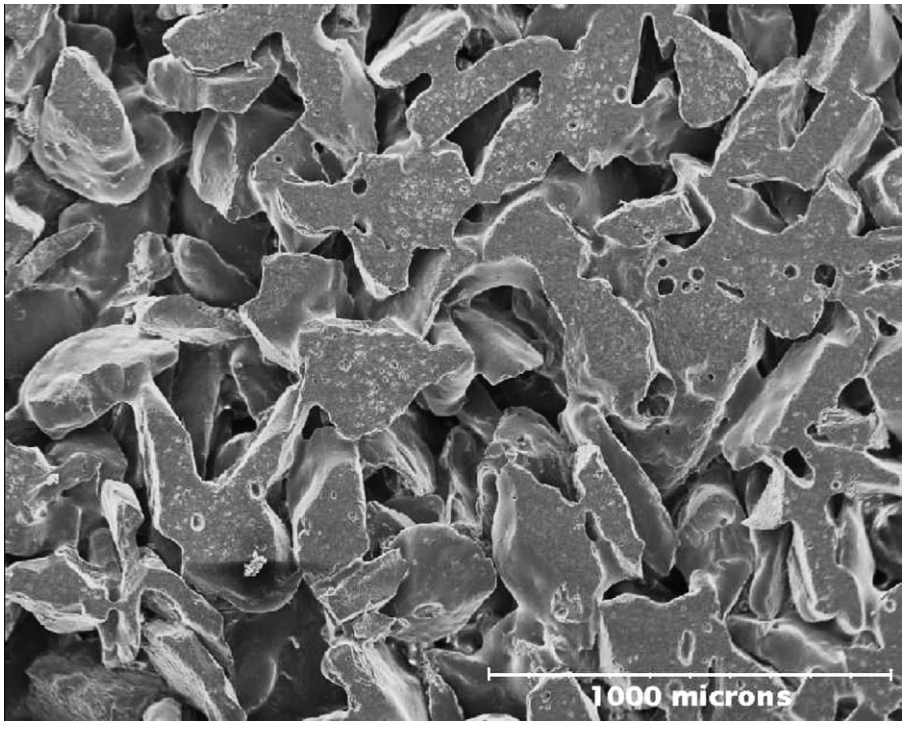

Fig. 3. Scanning electron micrography of the porous ceramic.

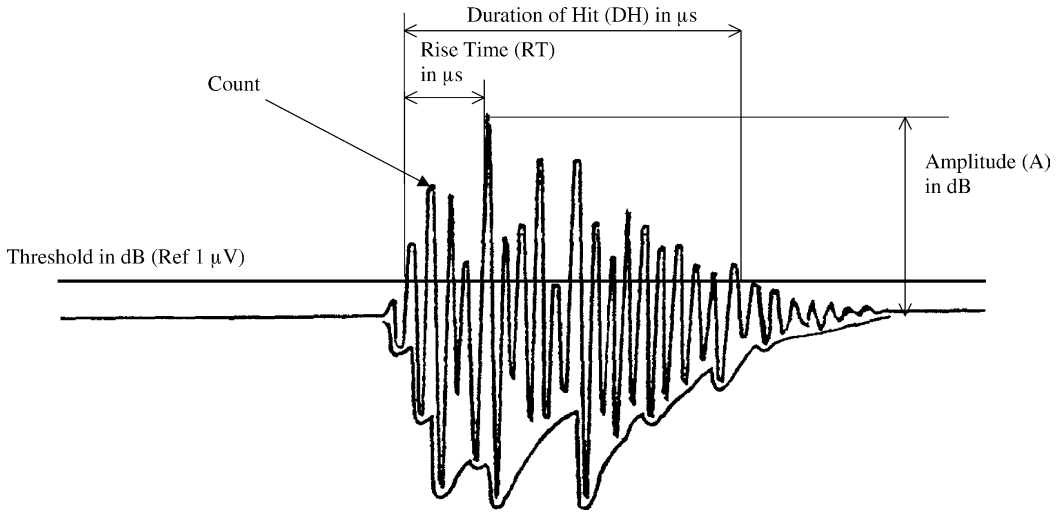

Fig. 4. Typical AE signal recorded with its associated characteristics.

subtract these parasite signals from the one recorded on the test sensor. The preamplifiers provide 40/60 dB gain (switch select) and operate with either a single ended or a differential sensor. A coupling fluid (Dough 428 Rhodorsil Silicone) is used to have an airless and flawless contact between the transducer and the specimen. For all the experiments, the samples are placed in a special chamber, where the temperature and the relative humidity (RH) are controlled (Fig. 5). Experiments were conducted either at atmospheric pressure (1 atm) or at a pressure of 10^{-2} atm.

Prior to experiments, the porous ceramic has been heated at 110 °C for 1 h and then stored under dry nitrogen at room temperature. This protocol has been applied in order to minimize the amount of water already adsorbed on the ceramic surface before testing. Two series of experiments have been carried out. In the first series, the ceramic is placed in different relative humidities of water and different pressures and is referred as "non-impregnated porous material". In the second series, the porous ceramic is impregnated with water under vacuum for a minimum of 4 h and is referred as "impregnated porous material".

4. Results and discussion

4.1. Results for non-impregnated porous material

Prior to AE experiments on the porous ceramic, a first test was carried out at 90% relative humidity and 1 atm on a specimen of similar dimensions made with stearic acid which is well known for its hydrophobic properties (no water adsorption). Only one hit was recorded during a period of 20 h. This result shows that our experimental configuration does not generates any parasitic signal.

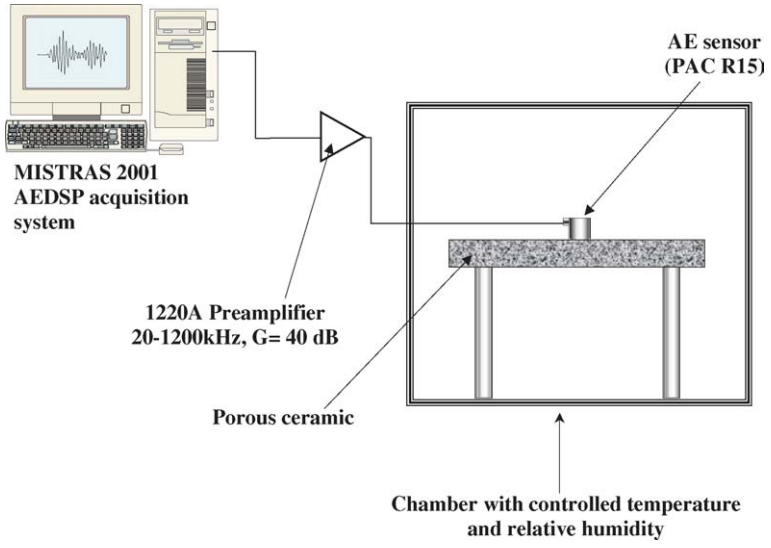

Fig. 5. Experimental setup for drying testing of a porous ceramic.

Table 1
AE features for non-impregnated porous media tested with different RH levels

Pressure = 1 atm	Hit rate (∂(Hit)/∂t) (hits/h)	Cumulative number of hits after 20 h
RH		
10%	1.4	25
40%	6.9	119
90%	32.9	657

4.1.1. *Influence of the relative humidity level under constant pressure (1 atm)*

The first testing campaign was performed on the ceramic—previously heated at 110 °C and stored under dry nitrogen—placed inside the chamber at atmospheric pressure (1 atm) with three relative humidities, namely 10, 40 and 90%. Each test has been performed three times and was found to be quite reproducible.

From these data, some interesting comments can be done. Firstly, we can note that for each humidity level, the acoustic activity starts from the very beginning of the test, even for the lowest RH level. A second observation is relative to the value of the cumulative number of hits (Table 1). According to Fig. 6, it seems that the total amount of hits during the test is related to the level of relative humidity. In fact the test under the highest RH level (90%) exhibits a maximum value around 650 hits after 20 h while the experiment under the lowest RH level (10%) reaches a maximum amount of 20 hits after the same duration. Thirdly, there is a fairly linear relationship between the cumulative number of hits and the time. Moreover, with respect to the hit rate (∂(Hit)/∂t), it is nearly five times higher for the highest RH level (90%) than for intermediate one (40%) and more than 20 times higher than for the lowest RH value (10%). A this stage of the study, it is important to remember that the porous material has been installed inside the testing chamber without being impregnated by any fluid and that, prior to AE measurements, it has been treated for 1h at 110 °C and kept at room temperature in neutral atmosphere (dry nitrogen).

Taking into account all these parameters, it seems that the acoustic emission is induced by an interaction between water molecules and the surface of the porous medium. Indeed, the more the RH level increases, the more the atmosphere inside the cell contains water molecules and the more water can be fixed on the surfaces of the pores. This phenomenon seems to lead to a linear dependence between cumulative number of hits and time. The water adsorption at the external surface of a pore is a process that changes the nature of the interface. In fact, the solid/vapour interface is replaced by a less energetic solid/liquid interface. This change leads to a release of energy (even at a very small level), which is transformed into mechanical waves propagating through the microstructure, and into thermal flow.

4.1.2. *Influence of the pressure level under constant relative humidity (90%)*

This testing campaign has been conducted on the same kind of porous ceramic with the same preparation protocol. The RH level is fixed at 90% and the pressure level in the chamber decreased from atmospheric pressure to 10^{-2} atm. Fig. 7a presents the evolution versus time of the acoustic activity of the porous ceramic under these two pressures. We assume that the pressure variation has no incidence on the deformation of the solid skeleton.

This figure shows one more time both the differences in maximum cumulated level and in hit rate (657 and 33 hits/h under atmospheric pressure, 47 and 2 hits/h for the test under 10^{-2} atm, respectively). The highest level in pressure corresponds to the highest values of the AE features. Another

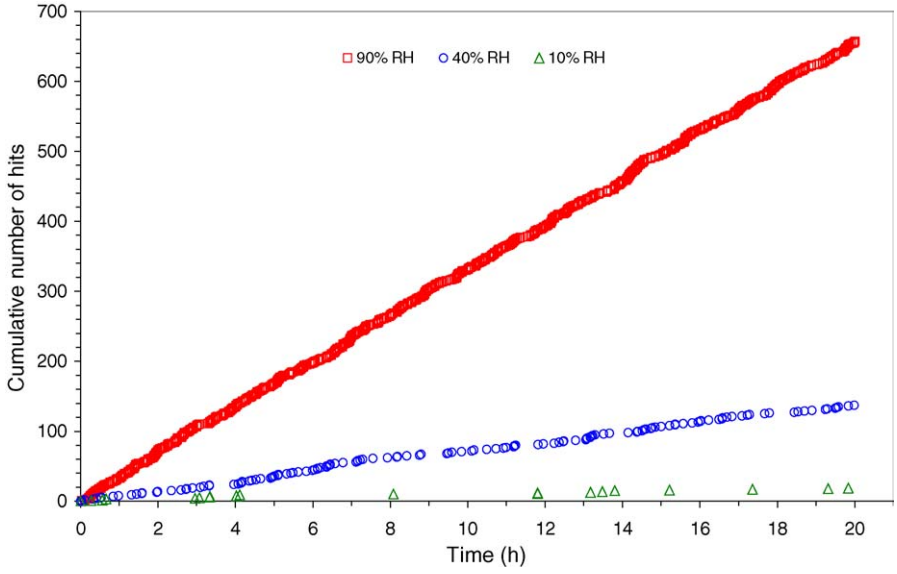

Fig. 6. Evolution of the acoustic activity of a non-impregnated porous medium for different levels of relative humidity (experiments conducted at 1 atm).

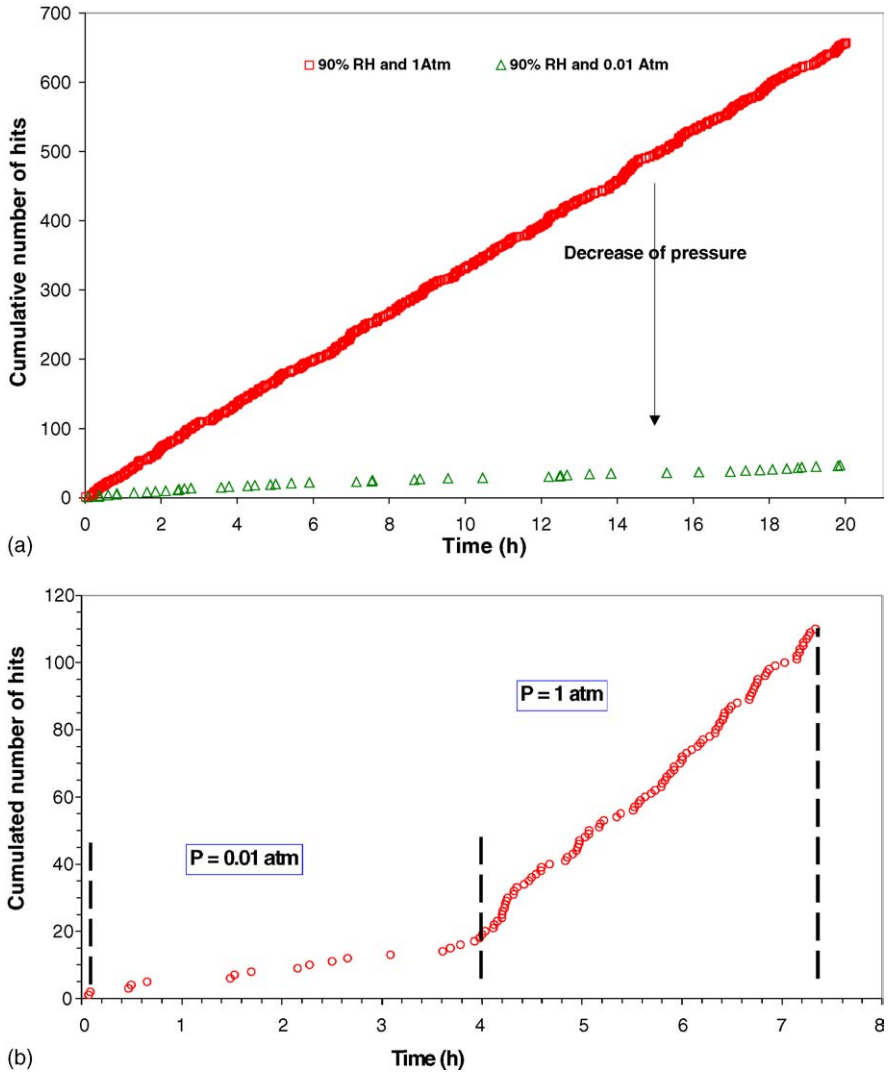

Fig. 7. (a) Evolution of the acoustic activity of a non-impregnated porous medium for different pressures (RH = 90%). (b) Evolution of the acoustic activity of a non-impregnated porous medium with two pressure levels: 0.01 atm for 4 h, 1 atm beyond 4 h (RH = 90%).

experiment was conducted under 90% RH (Fig. 7b). The pressure was initially equal to 0.01 atm and raised to 1 atm after 4 h. The value of the hit rate is clearly different before and after the pressure; it is equal to 4 and 27 hits/h, respectively. These values are of the same order of magnitude than those deduced from the experiments at a given pressure (2 hits/h under 10^{-2} atm and 33 hits/h under1 atm, Fig. 7a). According to the gas kinetics theory,[26] the flow F of molecules (in molecules/cm^2/s) hitting a unit area (cm^2) depends on the temperature T (K), the pressure P (Pa), the average molar weight M (in g/mol) of the considered molecules and the Avogadro number (N_a):

$$F = \frac{N_a P}{\sqrt{2\pi M R_g T}} \tag{9}$$

where R_g is the perfect gas constant.

According to this equation, an increase in pressure P will lead to an increase in the flow F of molecules. If we still consider the hypothesis that the adsorption of water molecules is closely related to the acoustic activity recorded during the test, the lower the pressure is, the lower is the recorded AE activity. In conclusion, the AE technique can be a useful tool to monitor adsorption of water on solid surfaces.

4.2. Results for impregnated porous medium

The porous ceramic is initially impregnated with water and placed on a piece of blotting paper in order to ensure a good emptying of the pores during the test. The experiments have been conducted at room temperature (23 °C), RH of 90% and under 1 atm. Prior to AE testing, the water weight loss of the porous medium has been measured under the same configuration. Fig. 8a presents the variation of the relative water weight loss as a function of time. As we can see here, the weight loss rate is rather high during the first hour (25.3%/h). After 1 h, the slope of the curve is slightly reduced and after

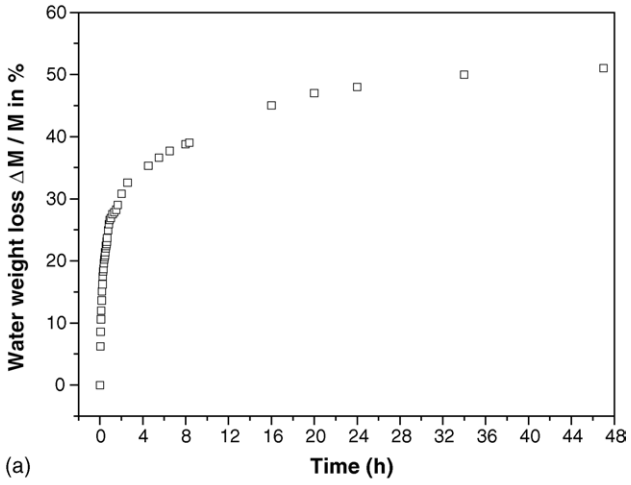

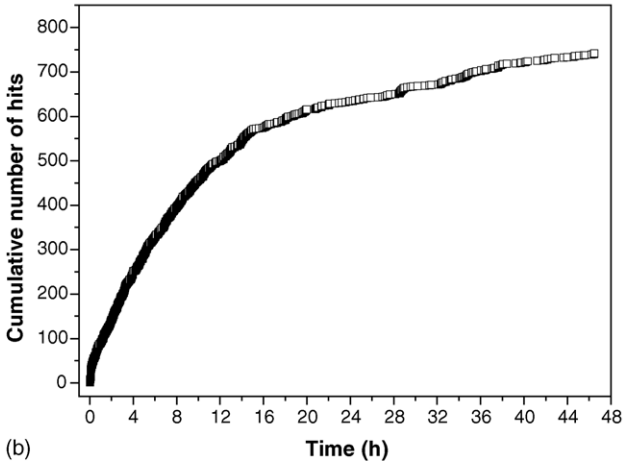

Fig. 8. (a) Evolution of the relative weight loss of water impregnated porous medium during drying (RH = 90%, P = 1 atm, T = 23 °C). (b) Evolution of the acoustic activity of a water impregnated porous medium during drying (RH = 90%, P = 1 atm, T = 23 °C).

48 h, the relative water weight loss reaches it maximum value, near 50%. The test is conducted at a high RH level (90%), it could explain the 50% of water which still remains in the porous ceramic after 48 h. Fig. 8b shows the evolution of the cumulated number of hits for the same sample under the same testing configuration. According to this figure, the variation of the acoustic activity seems to be related with the evolution of the relative water weight loss (Fig. 8a). In order to understand these variations, one has to consider the falling rate periods in the drying process. The meniscus retreats into the pore and the liquid is in its funicular state. During these stages, transport by liquid flow is possible, some diffusion occurs too and eventually evaporation (Fig. 1b). An hypothesis is that these two mechanisms could release energy and induce acoustic activity in the ceramic.

Coussy[26,27] detailed the thermodynamics of liquid transfer processes in porous media. The simplest approach is to consider the porous medium as a polyphasic continuum composed of an incompressible solid skeleton and a connected porous space partially saturated by incompressible liquid water (l) and an ideal mixture of water vapour (v) and dry air (a). The two principles of thermodynamics are applied to the elementary volume, which is an open system due to the fluid matter exchanges with the outside. Considering isothermal and poroelastic variations, the state variables of the system, namely the total stress tensor (σ) and the macroscopic free enthalpy per unit of mass of fluid (g) are closely related to the strain tensor (ε) and the mass variation (m), respectively. The macroscopic state equations of the porous medium can be defined as:

$$\sigma = \frac{\partial \Psi}{\partial \varepsilon}, \qquad g_{\mathrm{i}} = \frac{\partial \Psi}{\partial m_{\mathrm{i}}} \tag{10}$$

where Ψ is the global free energy of a unit volume of the porous medium and is considered as a thermodynamic potential. This free energy can be expressed as follows:

$$\psi = \psi_{\mathrm{SK}} + m_{\alpha}\psi_{\alpha} \tag{11}$$

with ψ_{SK}, the free energy of the skeleton which includes here both the free energy of the solid skeleton and the free energy of interfaces (γ_{SL}, γ_{SV} and γ_{LV}); m_{α} and Ψ_{α} are the mass of the fluid α per unit of volume and the free energy of the fluid α, respectively.

According to Coussy's work,[26,27] Ψ_{SK} can be identified as:

$$\Psi_{\mathrm{SK}}(\varepsilon_{ij}, S_{\mathrm{l}}, T) = \phi U(S_{\mathrm{l}}, T) + \psi_{\mathrm{S}}(T, \varepsilon_{ij}) \tag{12}$$

where S_{l} is the saturation in liquid of the porous body ($0 < S_{\mathrm{l}} < 1$), ϕ is the lagrangian porosity defined as the volume of the porous space by unit of solid body of the initial reference configuration.[1] U is the energy per unit of porous space and T the temperature. This equation clearly postulates that the global free energy of the system can be separated into two parts. A first term related to the energy of the interface ($\phi U(S_1,T)$) and a second term that more likely deals with the solid free energy ($\psi_{\mathrm{S}}(T,\varepsilon_{ij})$) on the basis that the solid is deformable. This last expression can be itself related to the elastic energy (w_{s}) of the solid:

$$\psi_{\mathrm{S}}(T, \varepsilon_{ij}) = w_{\mathrm{S}}(\varepsilon_{ij}) + f(T) \tag{13}$$

In terms of energy, this very short description is in accordance with the hypothesis of a close correlation between the onset of an acoustic emission activity and the different phenomena that occur during the drying process of a porous medium. Future works will deal with the frequency analysis of the acoustic emission signals in order to investigate the wave propagation through this multiphase medium, and in particular to check if it is possible to attribute specific characteristics to diffusion, flow, on one hand, and evaporation, one another hand. A simple estimation of hit rate from Fig. 8b shows that between 0 and 17.5 h, it decreases gradually while

[1] This lagrangian porosity ϕ is different than the euleurian porosity, n, that can be related to ϕ through the expression $\phi = Jn$ where J is the determinant of the homogeneous tangent transformation. The lagrangian porosity is the only one that, as the strain tensor, refers to the same system as each time.

it is fairly constant (equal to 5.9 hits/h) beyond 17.5 h. If we assume that, according to the results presented in Section 4.1.1, water adsorption, at pore surfaces, leads to a linear dependence between the cumulative number of hits and time, this phenomenon could explain the results on Fig. 8b beyond 17.5 h. In fact, during the second falling rate period, the vapour phase is in equilibrium with isolated pockets of liquid, a liquid film and the solid skeleton. It could be possible that some water molecules adsorb on the free solid surfaces thus leading to a decrease in the interfacial energy. Concerning the data on Fig. 8b for the period between 0 and 17.5 h, it could be attributed the diffusion and flow phenomena. Further work will be needed in order to check these various hypotheses.

5. Conclusion

Liquid transfer processes have been investigated by acoustic emission. This paper describes the monitoring of drying of a porous ceramic and the AE characterisation of several mechanisms involved in this phenomenon. The major concluding remarks are the following:

- AE technique is able to detect low energy processes acting at the molecule scale (adsorption of water at the pore surfaces).
- There is a correlation between the AE activity and the water weight loss of the porous medium during drying. These observations clearly show that this technique is able to characterise drying phenomena in a large-scale range (from nanoscopic to microscopic scale). Distinct AE signatures have been identified for the different processes.
- The hypothesis presented in the general theory of drying and its thermodynamical approach are in good accordance with the AE measurements. This result tends to demonstrate that the acoustic activity recorded during drying tests is directly related to the energy release of the system induced by the change in surface energy and the motion of the fluid.
- Lastly, the important advantage of this non-destructive, in situ and real time technique, is that it can be applied to follow the drying process of a large number of other materials, such as cement, mortars or concrete.

Acknowledgment

The authors want to thank the “Conseil Regional du Limousin” for its financial support.

References

1. Van Breugel, K., *Simulation of Hydration and Formation of Structure in Hardening Cement Based Materials*. PhD Thesis. Delft University of Technology, 1991.
2. Bentz, D. P. and Hansen, K. K., Preliminary observation of water movement in cement pastes during curing X-ray absorption. *Cem. Concr. Res.*, 2000, **30**, 1157–1168.
3. Hansen, K. K. and Bentz, D. P., Studies of hydration and drying in cement pastes by scanning X ray absorptiometry. In *Proceedings of Water in Cement Paste and Concrete—Hydration and Pore Structure Workshop*, 1999, pp. 107–114.
4. Scherer, G., Effect of drying on properties of silica gel. *J. Non Cryst. Sol.*, 1997, **215**, 155–168.
5. Nielsen, E., Einarsrud, M. A. and Scherer, G., Effect of precursor and hydrolysis conditions on drying shrinkage. *J. Non Cryst. Sol.*, 1997, **221**, 135–143.
6. Weinberger, R., Initiation and growth of cracks during desiccation of stratified muddy sediments. *J. Struct. Geol.*, 1999, **4**(21), 379–386.
7. Boutin, C. and Auriault, J. M., Dynamic behaviour of porous media saturated by a viscoelastic fluid. Application to bituminous concretes. *Int. J. Eng. Sci.*, 1990, **28**(11), 1157–1181.
8. Auriault, J. M. and Lewandowska, J., Modelling of pollutant migration with interfacial transfer: local equilibrium/non-equilibrium. *Mech. Cohe-Frict. Mater.*, 1997, **2**(3), 205–221.
9. Mironova, M., Gospodinov, P. and Kazandjiev, R., The effect of liquid push out of the material capillaries under sulphate ion diffusion in cement composites. *Cem. Concr. Res.*, 2002, **32**, 9–15.
10. Gospodinov, P., Kazandjiev, R., Partalin, T. and Mironova, M., Diffusion of sulphate ions into cement stone regarding simultaneous chemical reactions and resulting effects. *Cem. Concr. Res.*, 1999, **29**, 365–376.
11. Baroghel-Bouny, V., Mainguy, M., Lassabatere, T. and Coussy, O., Characterisation and idendification of equilibrium and transfer moisture for ordinary and high-performance cementitous materials. *Cem. Concr. Res.*, 1999, **29**, 1225–1238.
12. Hanzic, L. and Ilic, R., Relationship between liquid sorptivity and capillary in concrete. *Cem. Concr. Res.*, 2003, **33**, 1385–1388.
13. Shiotani, T., Bisschop, J. and Van Mier, J. G. M., Temporal and spatial development of drying shrinkage cracking in cement based materials. *Eng. Fract. Mech.*, 2003, 1509–1525.
14. Bazant, Z. P. and Raftshol, W. J., Effect of cracking in drying and shrinkage specimens. *Cem. Concr. Res.*, 1982, **12**, 209–226.
15. Bisschop, J., Pel, L. and Van Mier, J. G. M., Effect of aggregate size and paste volume on drying shrinkage microcracking in cement based composites. In *Proceedings of 6th International Conference on Creep, Shrinkage and Durability Mechanics of concrete (ConCreep6)*, 2001, pp. 75–80.
16. Bisschop, J. and Van Mier, J. G. M., How to study drying shrinkage micro-cracking in cement based materials using optical and scanning electron microscopy. *Cem. Concr. Res.*, 2002, **32**, 279–287.
17. Bourbié, T., Coussy, O. and Zinszner B., *Acoustique des milieux poreux* (in French). publication de l’institut français du pétrole, 1986. édition Technip, Paris.
18. Auriault, J. M. and Lebaigue, O., Acoustic waves in a mixture of fluids with capillary effects. *Int. J. Eng. Sc.*, 1989, **27**(10), 1253–1265.
19. Pauchard, V., Brochado, S., Chateauminois, A., Campion, H. and Grosjean, F., Measurement of sub-critical crack-growth rates in glass fibers by means of acoustic emission. *J. Mater. Sci. Lett.*, 2000, **19**, 2141–2143.
20. Ono K. and Huang Q., Pattern recognition analysis of acoustic emission signals. In *Proceedings of Progress in Acoustic Emission, Vol VII*, 1994. The Japanese Society For NDI, pp. 69–78.
21. Krietsch T. and Bohse J., Selection of acoustic emissions and classification of damage mechanisms in fibber composite materials. In *Proceedings of Progress in Acoustic Emission,Vol XI,1998*. The Japanese Society For NDI, pp. 80–87.
22. Ohtsu, M., Tomoda, Y. and Fujioka, T., Estimation of initial damage in concrete by acoustic emission. 1997. In *Proceedings of Fourth Far East Conference on NDT*, 1991, pp. 112–119.

23. Chen, H. L., Cheng, C. T. and Chen, S. E., Determination of fracture parameters of mortar and concrete beams by using acoustic emission. *Mater. Eval.*, 1992, 888–894.
24. Chotard, T., Smith, A., Rotureau, D., Fargeot, D. and Gault, C., Acoustic emission characterisation of calcium aluminate cement hydration at the early age. *J. Eur. Ceram. Soc.*, 2003, **23**, 387–398.
25. Scherer, G., Theory of drying. *J. Am. Ceram. Soc.*, 1990, **73**, 3–14.
26. Coussy, O., Thermodynamics of saturated porous solids in finite deformations. *Eur. J. Mech. A/Solids*, 1989, 1–14.
27. Coussy, O., *Mechanics of Porous Continua*. John Wiley and sons, 1995.